2021

Probing the Role of the Solvation Shell for the Iodine-Starch Complex Using Millifluidic Devices

Sarah E. Morley
Assumption University, Class of 2018

Benjamin J. Knurr
Assumption University, bj.knurr@assumption.edu

Recommended Citation

Morley, S. E.; and Knurr, B. J. (2021). Probing the Role of the Solvation Shell for the Iodine-Starch Complex Using Millifluidic Devices. *Journal of Solution Chemistry* 50: 833-850. https://doi.org/10.1007/s10953-021-01091-6

Probing the Role of the Solvation Shell for the Iodine-Starch Complex using Millifluidic Devices

*Sarah E. Morley and Benjamin J. Knurr**
Assumption University 500 Salisbury St. Worcester MA 01609
*Corresponding Author Email: bj.knurr@assumption.edu, ORCHID: 0000-0003-1812-8558

Abstract:

The iodine clock reaction and the resulting blue colored iodine-starch complex have been observed and studied for over a hundred years, but the structure of the product and mechanism by which it is formed are still not completely understood. The work presented here employs 3D-printed millifluidic devices as a reaction vessel that allows for spectral acquisition on a flowing iodine clock reaction in different aqueous alcohol solvents. UV-Vis absorption spectroscopy is used to probe the flow dynamics and study effects of the solvation environment of the iodine clock reaction under various solvent conditions. Bathochromic shifts of the product absorbances are observed when the solvent composition is changed from water to aqueous solutions of increasing amounts of methanol, ethanol, and 1-propanol. It is determined that the solvation network around the product complex helps to control the geometric and electronic structure of the complex and is easily perturbed by the addition of alcohol to the solution. The shifts are primarily attributed to a weakening of the solvation network around the complex rather than a decreasing polarity of the solvent and are due to interactions of the solvent with the starch portion of the complex. Finally, analysis of the laminar flow dynamics suggest that the complex may exist where solvent molecules have similar velocities and thus are able to form a stable solvation network and that triiodide may form slightly prior to the complex. The insights gained from these observations can help guide modeling of the iodine-starch complex and provide benchmarks for the expected effects of different solvents on the electronic structure of the product complex.

Keywords: Solvation, Solvent Effects, Spectroscopy, UV-Vis, Iodine-Starch

Declarations:

Funding: This work was supported by the Provost's office at Assumption University.

Conflicts of interest/Competing interests: The authors declare no conflicts of or competing interests.

Availability of data and material: Not applicable

Code availability: Not applicable

Authors Contributions: The manuscript was written through contributions of all authors. All authors have given approval to the final version of the manuscript.

Acknowledgements: The authors wish to thank the Assumption University Biological and Physical Sciences department for their support of this work and the opportunity for undergraduate student research experiences.

1 Introduction

The iodine clock reaction has been studied for many years, as it creates a novel product complex that perplexes and fascinates scientists to this day [1–5]. The nature of the product species (vivid dark blue) in stark contrast to the reactants (all colorless) makes for an exciting visual change. In addition, the reaction is in a unique class of reactions known as clock reactions, in which the final product formation is time-delayed due to the presence of a "clock species." The clock species consumes an intermediate and prevents final product formation until the clock species itself is exhausted. Thus, the final product(s) can form with a time delay which is dependent on the initial amount of the clock species. Since there are multiple variations of this reaction, a single type was chosen as the focus of this study. The following reaction diagram outlines the selected non-oscillating iodine clock reaction, where the time between the first two steps is controlled by the concentration of metabisulfite ($S_2O_5^{2-}$).

$$\underbrace{IO_3^- + S_2O_5^{2-}}_{\text{Colorless}} \rightarrow I^- + I_2 + \text{Starch} \rightarrow \underbrace{\text{Iodine Starch Complex}}_{\text{Blue}}$$

The reaction itself has been known since 1886 [6, 7] and both the non-oscillating and oscillating versions [8] of the reaction are often used in chemistry lectures and labs. The demonstration is frequently presented to highlight aspects of chemical kinetics, such as the existence of non-elementary rate laws and time-delayed chemical reactions [2, 9]. Even though this reaction has garnered attention and study from chemists at many different levels for many years, there remain some surprising knowledge gaps in the structure and formation pathway of the product complex including what role the solvent has in influencing the product complex [10]. Insights into the formation and properties of the product complex may reveal novel structures of iodine (similar to I_3^-, I_5^-, I_7^-, polymeric chains of iodine, etc.) and aid in the modeling and description of the electronic structure of complexes containing starches such as amylose.

Understanding the role solvent can have in influencing the structure of the complex as well as interactions between the different pieces of the iodine-starch chromophore can be useful for predicting the interactions present in larger and more biologically relevant chromophores.

Perhaps the most elusive piece of information is the structure of the iodine-starch complex that is formed over the course of the reaction. Historically, the focus has been on the iodine species present within the complex [1–3]. There has been a long series of debates concerning potential candidates such as I^-, I_2, I_3^-, I_5^-, and different combinations of these and other various iodide species [11–13]. Unfortunately, there has yet to be a definitive answer as to the structure of this complex. This question is complicated further since the properties of the iodine-starch complex are quite different from the properties of either of the individual starch or iodine species thought to be initially present when the complex forms. The large structure and aqueous nature of the reaction make computational studies of the iodine clock reaction and its potential products quite challenging as well [14, 15]. Accurately modeling the soluble starch and the solvation environment, all while attempting to predict the structure of the iodine component of the complex is a challenging problem. Theoretical studies have been performed to attempt to model and predict molecular properties in various polar and non-polar solvent environments, but this remains a difficult problem to tackle [16–20]. Experimental observations of solvatochromatic shifts in different solvation environments indicate that the solvent environment often plays a critical role in influencing the physical and electronic structure of the solute [10]. Consequently, numerous studies have focused on accurately and efficiently describing solute and solvent structure in various solvation environments [21–24]. However, there is little prior research on the effects of the solvent environment on the iodine-starch complex leaving a gap in the knowledge of this species in aqueous solution.

Previous attempts at solving for the structure of the complex and its solvation environment have focused primarily on using different spectroscopic techniques such as UV-Vis and vibrational Raman to gain information on the product complex. The primary focus has been on visible absorbances around both 400 and 650 nm and on a set of Raman shifts observed around 170 cm^{-1} with a focus on identifying the spectroscopically active structure [1–3, 25]. There has been much debate about the origins of these spectral features, particularly with respect to the structure of the iodine within the complex. The general consensus had been that polyiodides, such as I_3^- or I_5^-, are interacting with the starch to generate the blue complex [26]. A recent study by Madhu et. al. suggested that there may be an infinite polymeric structure of neutral/reduced iodine where the iodine is in nearly linear chains between columns of starch molecules [5]. However, the effects of the solvent environment to influence the species formed or the structure of that species have not been investigated.

The work presented here reports on aspects of the solvation shell around the iodine-starch complex and the effects that changing the solvent environment has on the absorption properties and structure of the product complex. Millifluidic devices were employed to acquire *in situ* spectra as the reaction progressed. Changes in the complex formation due to changes in the solvent composition may suggest particular structures or mechanisms by which the complex is formed. Additionally, the degree of solvatochromatic shift observed during incremental changes to the solvent environment may also indicate specific solvent–solute interactions and elucidate more information about the electronic transition(s) involved in the rich blue color of the complex and the role of the solvent in controlling the shape of the complex.

2 Experimental

2.1 Experimental Design

All of the reactions described here were carried out in 3D printed millifluidic devices fabricated using ABS plastic (Fig. 1). Millifluidic devices were employed to ensure a fresh sample of the solution was always being probed and to enable the option to analyze the absorbances in the context of the flow profile. Each linear flow region of the device will be referred to as a duct and ordered from inlet to outlet totaling seven ducts. The flow ducts have a square cross-section of 1.5 mm × 1.5 mm. The two holes in the top of the device were tapped in order to accommodate tubing fittings and ferrules. The initial 1.2 inches of the first duct was designed as a pseudo-helical static mixer composed of a series of X-shaped obstacles in an alternating pattern (Fig. 1a). This static mixing design can be found in large scale industrial flow mixers [27] and was adapted to fit the scale of the devices and be compatible with small-scale 3D printing. Mixing is achieved by alternately forcing the top and bottom and the left and right of the flow together. See the *Supporting Information: 3D Printing and Device* for more detail and the CAD design file.

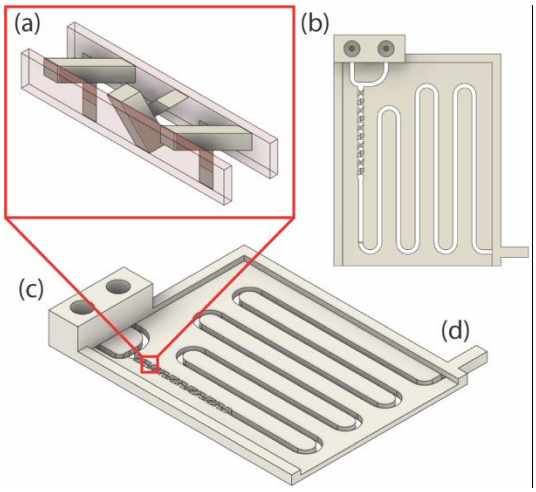

Fig. 1 A schematic diagram of the millifluidic device: (a) the pseudo-helical static mixer containing ten crosses total, (b) top view of the reaction vessel showing the flow path of the solution, (c) tapped inputs for tubing carrying reaction solutions, (d) output flow spout

Quartz microscope slides (5.08 × 7.62 × 0.1905 cm) were attached to the top and bottom of the device using epoxy. Quartz slides were used to ensure that absorbances could be collected over the full visible and UV spectrum available from the experimental light source. To measure the UV-Vis spectrum of a flowing reaction, the device was mounted above a small optical table to allow for access to both the top and bottom of each duct (Fig. 2). The device holder was attached to four stacked linear micrometer stages (the bottom one mounted to the optical table), each with 1 inch of linear travel (0.001 in graduations). A total of 4 in^2 of travel was achieved by mounting two micrometer stages in each of the *x* and *y* directions. The end of the linear portion of the first duct contained a thin plastic bar on the bottom of the duct which was used to align the zero position of the micrometers (discussed further in *Supporting Information*). The bar was removed prior to use so it would not impede or alter the laminar flow in the device.

Two fiber-optic cables (0.6 mm diameter) were mounted facing each other with a gap of approximately 7 mm in between, so that the millifluidic device fit between them without touching the tip of either cable (Fig. 2). The lower cable was connected to an Avantes AvaLight-DHc UV-Vis light source (200 nm to 1100 nm) and the upper fiber-optic connected to an Avantes SensLine AvaSpec-ULS2048x64 spectrometer (200 nm to 1100 nm, resolution of 1.4 nm FWHM). The device was translated while the fiber-optic cables remained stationary to ensure consistent alignment, while simultaneously accessing the entirety of the reaction vessel. Transmission spectra were collected and later converted into absorbance spectra. Reference spectra were recorded over the entirety of the device. Temperature control of the device and the solutions contained within was not possible during spectral acquisition without obscuring the optical pathway through the device so all spectra were acquired at ambient temperature which fluctuated between 16 ˚C and 21 ˚C. For more detail, see the *Supporting Information*.

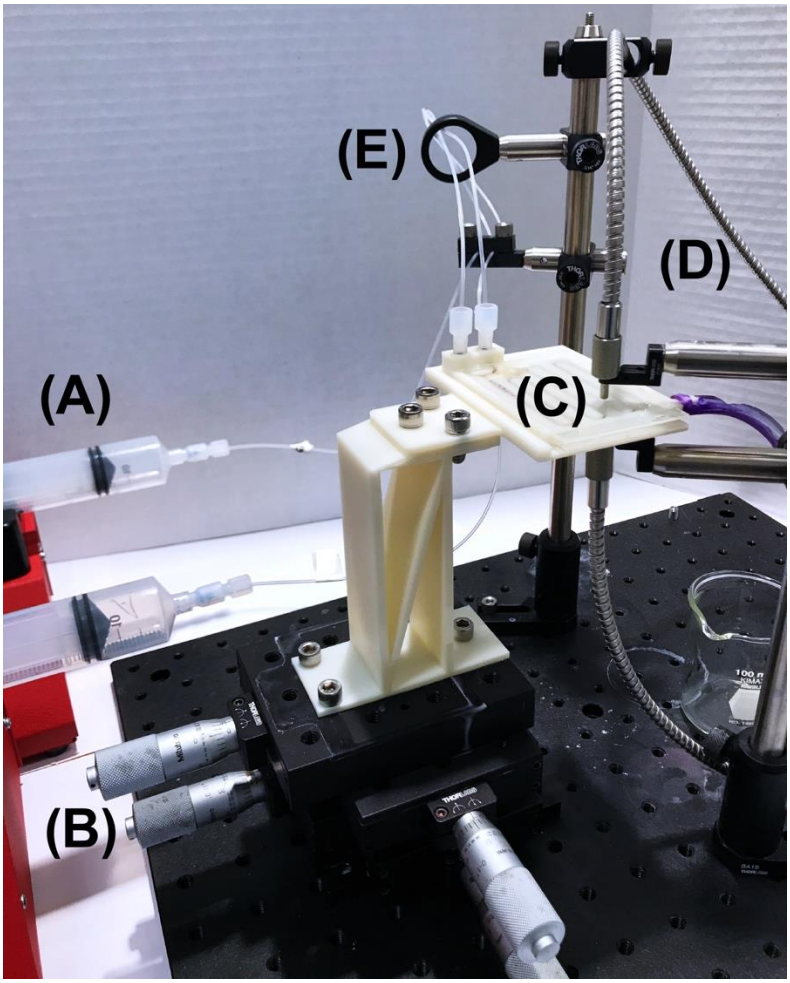

Fig. 2 A picture of the experimental setup: (A) the syringe pumps, (B) micrometer stages used to translate the device, (C) the millifluidic device shown in Fig. 1, (D) the fiber-optic cables connected to the light source and spectrometer, (E) mounts used to prevent kinks and strain in both tubing and fiber-optic cables

2.2 Solutions Used and Spectral Acquisition

Each iodine clock reaction involved two reactant solutions, referenced as solution A and B. Solution A contained 0.0200 $mol \cdot L^{-1}$ potassium iodate and solution B contained the starch, sodium metabisulfite (clock species), and sulfuric acid [4, 9, 28]. While the solvent compositions were varied, the solutes in all A and B solutions were prepared in the same manner. The solvent compositions tested were deionized water and aqueous solutions of 5%, 10%, 15%, 20%, and 25% methanol, ethanol, and 1-propanol by volume. The source and purity of the reagents used are given

in Table 1 and full details of the composition of each solution are given in the *Supporting Information*.

Table 1 Source and purity information for all chemicals used this these experiments.

Chemical	CAS no	Source	Purity
Potassium Iodate, AR	7758-05-6	Mallinckrodt	99.5 %
Starch, soluble	9005-84-9	Sigma-Aldrich	ACS Reagent
Sodium Metabisulfite	7681-57-4	J.T. Baker	97.9 %
Sulfuric Acid	7664-93-9	Pharmco-AAPER	95.0 – 98.0 %
Methanol	67-56-1	Sigma-Aldrich	≥99.9 %
Ethanol	64-17-5	Pharmco-AAPER	99.5 %
1-Propanol	71-23-8	Sigma-Aldrich	99.5+ %

Portions of solution A and solution B were transferred into syringes mounted on separate New Era NE-1000 automated syringe pumps, which were set to a flow rate of 0.25 $mL \cdot min^{-1}$. The solutions were pumped through plastic tubing and into the device (Fig. 2) and the system was given 5 to 10 minutes to achieve stable flow conditions before any spectra were collected. UV-Vis absorbance spectra were taken every 0.1 in along the device ducts, which equates to approximately 0.7 s of reaction time between scans (as related to the flow in the center of the duct). Spectra were not taken in the curves of the device to avoid issues with determining the exact center time of the point at which the spectrum was taken. A representative background spectrum was created for the specific solvent composition of each reaction by flowing only the solvent through the device, taking a set of absorbance spectra across the entirety of the device, and averaging the resulting spectra. The spectra were analyzed using OriginLab software and full sets of all spectra and backgrounds were recorded on at least two different days with freshly made reagents to ensure reproducibility of the spectra.

3 Results and Discussion

3.1 Spectra and Starch Solubility

If iodide and iodine are introduced into a solution of dissolved soluble starch, the previously colorless starch solution will become a vivid dark blue. The rate at which iodine forms from IO_3^- can be controlled by the addition of metabisulfite ($S_2O_5^{2-}$) or a similar oxidizer. The $S_2O_5^{2-}$ in the presence of an acid decomposes to HSO_3^-, which acts as a sink for generated I_2 by reducing it to I^-, thus preventing the formation of the complex and the blue color appearing in solution. When the metabisulfite has been consumed, iodine can then persist in solution and the blue color manifests as the iodine-starch complex forms. This general reaction scheme has been outlined previously by Lambert et. al. [4] (Fig. 3).

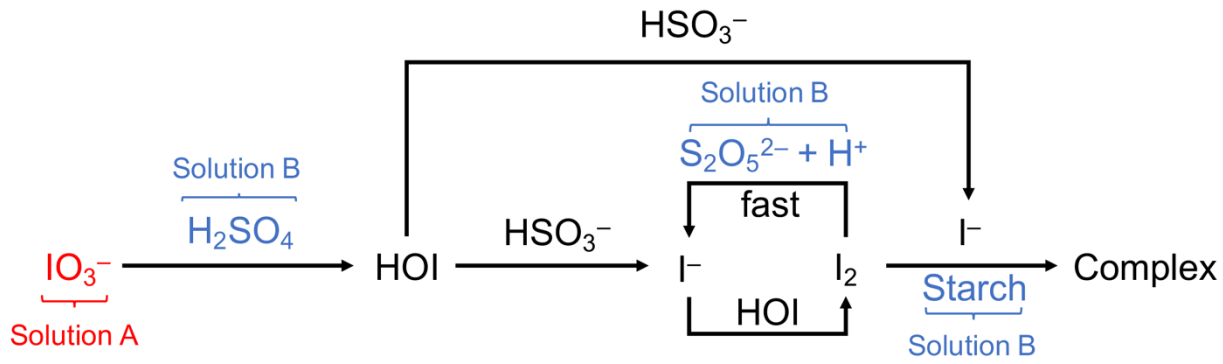

Fig. 3 The general reaction scheme for an iodine clock reaction: (red) species in Solution A, (blue) species in Solution B (see Experimental Methods for details)

For each solvent mixture studied, a waterfall plot of all the absorption spectra was made to observe the time(s) during which product formation occurred. Figure 4 shows the waterfall plot of the iodine clock reaction carried out in water. As is apparent in Fig. 4, a large visible absorption begins to appear centered about 650 nm, which corresponds to the formation of the blue colored iodine-starch product as the reaction progresses. The two absorbances around 350 nm to 300 nm are attributed to the triiodide ion and the pentaiodide ion respectively, and the shoulder at ca. 480

nm is in agreement with the absorbance spectrum of aqueous I_2, all known products of this reaction [11]. The off-scale peak at 220 nm is UV absorption by excess reactant IO_3^-. Full waterfall plots for all solvent mixtures tested are shown in *Supporting Information*.

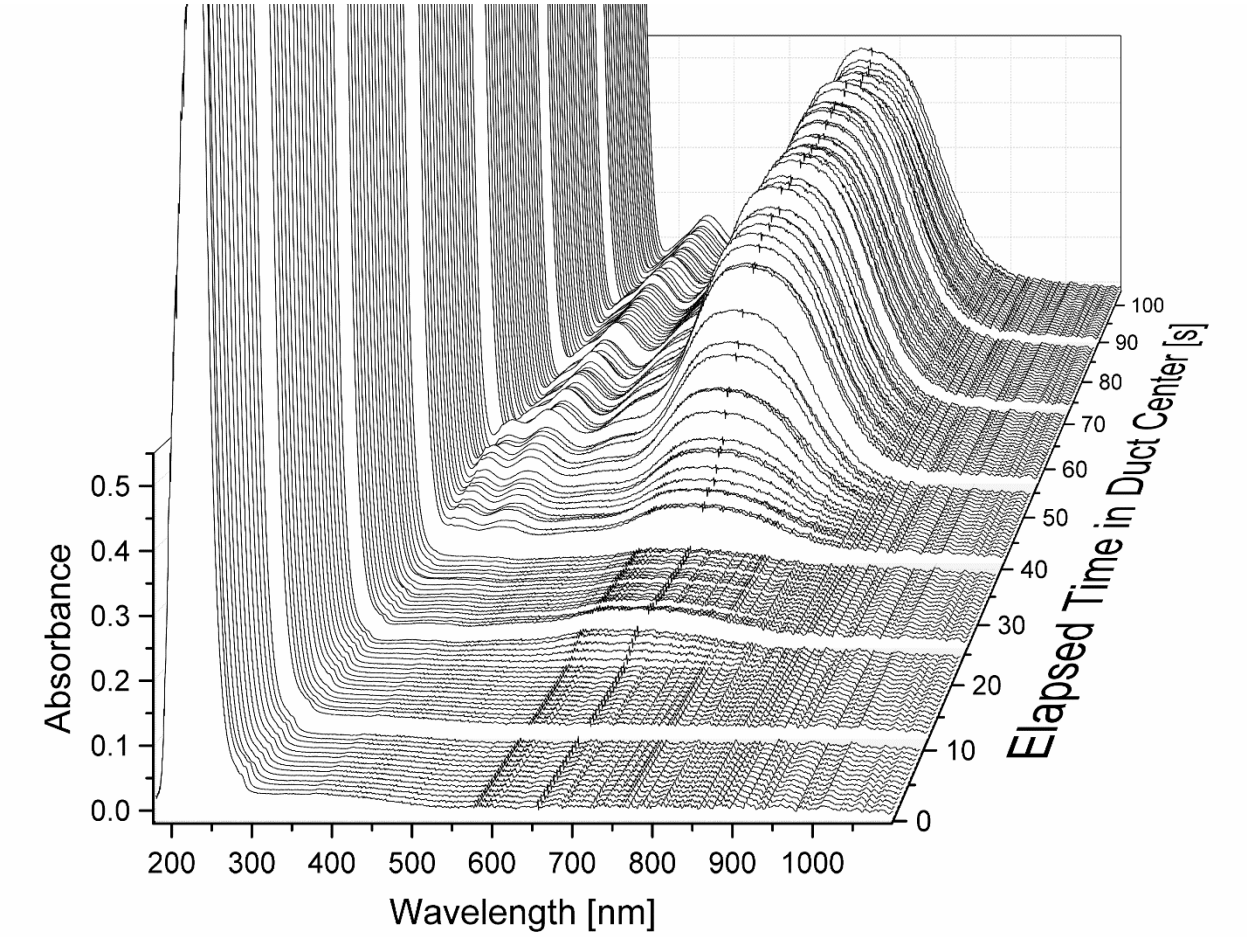

Fig. 4 Waterfall plot of the acquired UV-Vis spectra of the iodine clock reaction with a solvent of water: the off-scale absorbance around 220 nm is due to a large concentration of unreacted IO_3^- and gaps between sections result from no spectra being collected in the curves of the device

The time between mixing and observation of the blue color is controlled by the initial quantity of metabisulfite relative to the amount of IO_3^- initially present. If a larger quantity of metabisulfite is present, the clock reaction will take longer to form the starch-iodine product. All of the reactions reported here used equal initial amounts of all reactant species and only varied the composition of the solvent. As can be seen in Fig. 4, the 645 nm absorption in the millifluidic

reaction vessel becomes quite pronounced around 45 – 50 s elapsed reaction time and is generally in agreement with the observed completion time of the same reaction mixture in benchtop glassware. This observation suggests that the reaction is occurring similarly in the reaction device as it would in a bulk solution. However, the rate of absorbance increase due to the product species formation must be considered in the context of the laminar flow dynamics of the millifluidic device.

Before discussing the results further, it is necessary to address the solubility of the starch in the various solvent environments tested here. The solubility of the starch decreased in direct correlation to either an increase in alcohol concentration or an increase in the size of the alcohol (i.e. chain length). These observations are to be expected since the starch used in this reaction, while slightly soluble, does not readily dissolve in water like many polar or ionic molecules would. Rather, starch molecules become encased in a water network that holds them in solution [29]. If this network is disrupted by introducing less polar molecules (e.g. alcohols) that weaken the solvent network, the starch can break out of the network and precipitate more easily. Additionally, if the already large species being solvated increases in size (e.g. the iodine-starch complex forms or multiple starch molecules aggregate together), the solvation network must also grow, leading to increased constraints on what constitutes an effective solvation network resulting in decreased solubility.

As a result of the sensitive solubility of the starch, spectra collected for solutions of 20% 1-propanol and 25% for all alcohols resulted in many clogged millifluidic devices, and the absorbances measured over time were difficult to interpret for those solvent compositions. Visible precipitation of the starch occurred after the mixing region and, over time, the amount of precipitated starch was observed to slowly increase. Additionally, some attempts were made to

perform this reaction with aqueous 1-butanol as a solvent, but the starch insolubility could not be overcome even at low 1-butanol concentrations. Increased temperatures may have improved solubility with 1-butanol but would have made comparisons of spectra collected at different temperatures inappropriate. Some solvent mixtures required solution B (the starch containing solution) to be made with only a 10% alcohol concentration and solution A with a larger alcohol concentration so that the resulting mixture of the two would yield the desired alcohol concentration. This was done to ensure that all solutions initially contained equal amounts of starch and that minimal starch precipitation would occur within the device over the course of the reaction. While this technique did initially improve the solubility of the starch and the complex, in solutions with 15% aqueous alcohol or greater enough starch still precipitated such that many devices became clogged (requiring the experiment to be rerun) or ducts were obscured to the point where data acquisition was no longer feasible. Additionally, a decreased absorbance signal to noise ratio was observed in solutions with larger alcohol concentration and observed precipitation (see *Supporting Information*).

When the starch precipitated out of solution it visibly blocked portions of some ducts within the reaction device, obscured the ability to acquire spectra at some locations (elapsed reaction times), and in some instances resulted in premature product formation (e.g. see *Supporting Information* Fig. S5 and Fig. S10). If a spectrum could not be measured at a location, the micrometers were adjusted to find a suitable location along the center of duct or the point was skipped for that experiment. Excessive precipitation also affects the laminar flow dynamics within the duct by introducing obstacles to the flow. These effects are discussed further in the following section. All solutions of 1-propanol did show some precipitation owing to the destabilizing nature of 1-propanol to the solvent network and as a consequence, the laminar flow analysis discussed in

the following section is not a complete representation of the flow when 1-propanol was present in the solution.

3.2 Flow Analysis

The flow in the device after the mixing region is laminar, as is expected for most millifluidic and microfluidic devices. The Reynolds number (*R*) is calculated to be around 2 for the various solutions under the experimental conditions (see *Supporting Information* Table S2) and laminar flow is generally achieved when *R* is < 2000 [30]. With laminar flow, the liquid in the square pipe (or duct) of the device is separated into sheets or layers that each flow with their own characteristic velocity. The velocity of a sheet is dependent on its distance from the walls of the duct and the laminar planes in the center of the duct will move faster than those near the walls. The velocity at any given point in the millifluidic duct can be calculated using equations derived from solutions to the Navier Stokes equation employing the no-slip boundary conditions (velocity is zero at the walls of the chamber) [30, 31]. The resulting collection of velocities represents the velocity or flow profile of the fluid. The calculations discussed here utilize a unitless velocity profile where the *z* axis is in the direction of the flow and the *x* and *y* axes correspond to the width and height of the duct respectively (see Fig. 1). Due to the boundary conditions, the center of the duct has a relative velocity of 1 while the walls have a velocity of 0 and there is a symmetric 2D distribution of velocities between the center and the walls of the duct (calculation details are in *Supporting Information*). A heat map of the velocity profile is shown in Fig. 5.

To predict how the laminar flow profile will affect the observed absorbance values over time, the volume of the duct being probed was defined as a cylinder with a diameter of 0.6 mm (the size of the detection optical fiber) that spanned the full height of the duct (1.5 mm). This volume was then divided into approximately 30,000 individual regions, each with a volume of

0.025^3 mm^3. The regions were distributed to create the circular cross section of the probe volume and the cross sections were stacked to recreate the entire cylindrical probe volume. The elapsed reaction time was calculated at the center of each region using the relative velocities determined by the flow profile and attributed to all species present in the volume of that region. By combining all of the regions together, a map of the elapsed reaction times of the entire probe volume was created. Finally, by applying a completion time for the reaction, when products have been formed which was determined based on the absorbances measured (see Fig. 5), it was assumed that the species within a region calculated to be at or beyond that completion time would have reacted and generated products. Since the formation of products is instantaneous on the timescale of this experiment, the completion time was determined as the time when the total absorbance of the iodine-starch complex was no longer appreciably increasing (e.g. 55 sec for 5% methanol solution shown in Fig. 5). The expected total normalized absorbance was then calculated by dividing the number of regions that had reacted by the total number of regions in the probe volume. The predicted normalized absorbances ranged from 0 to 1, indicating the total fraction of molecular reactions that had occurred. Based on the elapsed time of the center point of the probe volume, the elapsed time of each region could be calculated to create a prediction of the absorbance vs. time at the center of the flow duct data collected in the experiment (details of calculations are shown in *Supporting Information*).

To compare the flow model to the experimental absorbances, the average absorbance around the λ_{max} (± 5 nm) of each of the three product species (iodine-starch complex, I_2, and I_3^-) were calculated. This averaging was done for each solvent configuration from a reaction time where there was no observable absorbance until the absorbance had reached a stable maximum absorbance. The experimental absorbances were baseline corrected and normalized to the average

maximum absorbance observed for their respective product species in the given solvent (e.g. measured absorbances from 60 to 80 seconds in Fig. 5). The resulting normalized experimental absorbance of the iodine-starch complex was plotted against the predicted model absorbances and can be seen in Fig. 5 for the 5% methanol solution (comparisons of the flow model to other solutions are shown in *Supporting Information*).

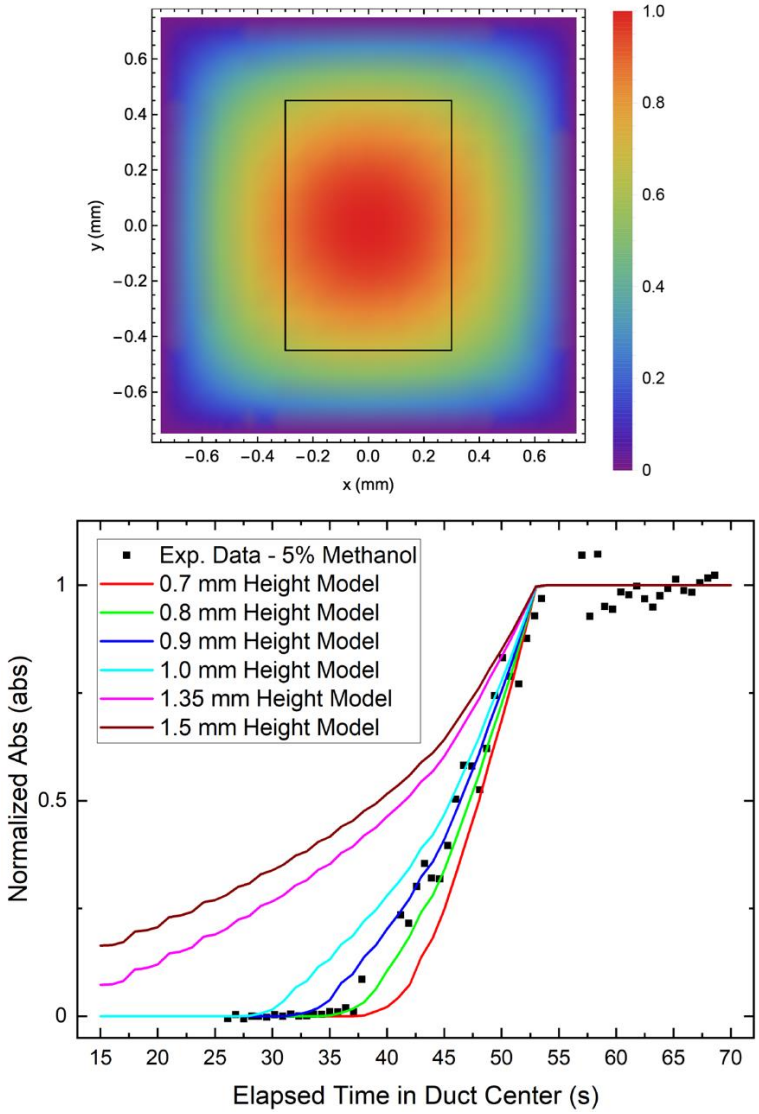

Fig. 5 (top) Calculated heat map of the relative velocities for the laminar flow profile with the 0.9 mm tall probe volume indicated by the black box, (bottom) comparison between experimental absorbance of iodine-starch complex with a solvent of 5% methanol by volume (black squares, uncertainty in time is the width of the black squares, ±0.3 s) and model absorbances for probe volumes of different heights

It is immediately apparent from the comparison that the model absorbances do not agree with the observed experimental absorbances when treating the full height of the duct for the probe volume (see brown full height trace in Fig. 5). Specifically, the model predicts that absorbances should be observed much earlier than were measured in the experiment and that the absorbances should increase more gradually than what was observed. The profile of the full height model absorbances is due to the speed of the laminar flow planes near the duct walls. The relative velocity is approximately 0 at and near the walls of the duct resulting in calculated elapsed reaction times reaching the threshold time for completion of the reaction early on in the device. The model therefore predicts a slowly increasing layer of product species originating at the walls of the duct, since the model assumes that the solution is homogeneous throughout the duct and each of the lamina is unperturbed. The experimental data clearly shows that absorbance of the product species is first observed much later and increases more rapidly that the model would predict. If the height of the probe region is symmetrically decreased from the full height of the duct, essentially assuming that absorbing molecules have low concentration near the walls, the model begins to agree more with the experimental data. Only the height was adjusted since the probe volume extended from the top to the bottom of the duct and the width/circumference was defined by the size of the fiber optic cable (0.6 mm diameter). Multiple heights were tested (1.5 mm, 1.35 mm, 1.0 mm, 0.9 mm, 0.8 mm and 0.7 mm shown in Fig. 5) and when the probe volume was limited to a height around 0.9 mm there is generally good agreement between the predicted and experimental absorbances (both in Fig. 5 and for other solvent compositions shown in *Supporting Information*).

There are seemingly two possible explanations for this adjustment to the model. First, the presence of turbulent flows in the duct may exist. The process of 3D printing the millifluidic devices does not leave the walls perfectly smooth. As a consequence, the outer most laminas will

experience a small amount of constant turbulence and cause some additional mixing between those laminas preventing iodine-starch molecules from sitting on the walls of the duct. Similarly, when some starch precipitates it will also create small turbulent regions near the walls of the ducts that will also cause mixing of the outer laminas. This additional turbulence should decrease the number of molecules that are virtually stationary near the walls and instead force them more toward the center of the flow.

Second, due to the small scale employed in milli- and microfluidic devices, the velocity differences between laminar planes near the walls of the duct will be quite large given that within about 0.2 mm of the wall (13% of the total height or width) the relative velocity will have increased to half of the maximum (see Fig. 5). This large change in velocity may create an unstable solvation environment near the walls of the duct where one side of a molecule – especially a large one like starch or the iodine-starch complex – will have relatively slow-moving solvent molecules while the other side will have molecules moving much faster. If molecules are to remain in a stable solvation environment, they may naturally migrate toward the center of the flow profile. This consideration of the solvation environment also suggests that a decrease in the height of the probe volume would be appropriate to account for a more likely location of the absorbing species. It should be noted that at a probe volume height of 0.9 mm, the height is still larger than the width (shown in Fig. 5) so there are absorbers beyond the width of the probe volume that are not being measured but are following the same flow dynamics.

The absorption peaks of I_2 and I_3^- were also compared to the model and it is apparent that the experimental absorbances by all the product species are occurring within a similar region of the duct (see Fig. 6). All three product species absorbances increase at about the same rate in each reaction. These observations indicate that all absorbing species are experiencing similar flow

environments within the duct. The absorbances for 5% 1-propanol in Fig. 6 also show that the starch solubility issues with 1-propanol dramatically change the flow conditions (discussed in the previous section) and thus makes the flow model less applicable to all solutions containing 1-propanol.

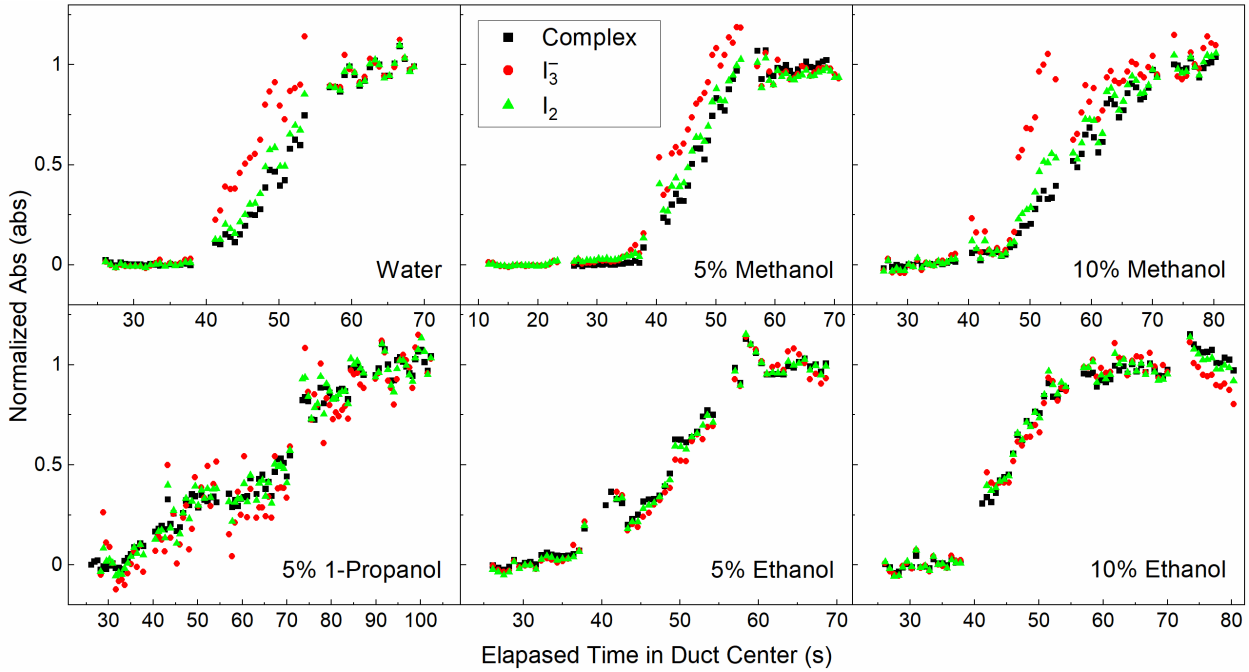

Fig. 6 Comparisons of individual species' absorbances for the iodine-starch complex (black squares), iodine (green triangles), and triiodide (red circles) for various solvent configurations as a function of time where uncertainty in the reaction time is the width of the symbols (±0.3 s) and starch precipitation in solutions containing 1-propanol changed the absorbance pattern

The comparison of the absorbance increases in Fig. 6 show that the I_2 and the iodine-starch complex absorbances are very similar across all solvent compositions. This observation is at least somewhat influenced by the spectral overlap of the two absorbance peaks, resulting in the measured absorbance by I_2 being impacted by the iodine-starch complex absorbance. However, the absorbance of I_3^- begins and reaches its maximum about 5 seconds prior to the iodine-starch complex in water and aqueous methanol but is generally concomitant with the iodine-starch complex in ethanol and 1-propanol. Considering that both the iodine-starch complex and I_3^- can

form once I_2 becomes present (i.e. the clock step of the reaction is complete) it appears that formation of I_3^- is initially the preferential pathway in solutions with a more polar solvent composition. This may be an equilibrium driven process since the equilibrium constant for the formation of I_3^- from I_2 and I^- in aqueous solutions has been measured previously to be around 700, indicating a general preference for the formation of I_3^- in a solution with relatively small amounts of I_2 and large amounts of I^- [32, 33]. However, when the solvation environment becomes less polar with the introduction of high methanol concentrations or other less polar solvents (e.g. ethanol and 1-propanol), this distinction in I_2 to I_3^- conversion mostly disappears (see Fig. 6). The change in the timing of I_3^- formation is attributed to the less polar solvation environment being able to more easily sequester the I_2 and decrease the interaction between I^- and I_2.

These observations indicate that when carried out in a primarily aqueous environment, the iodine clock reaction initially produces triiodide anions prior to forming the complex. Therefore I_3^- ions are present, in addition to I_2 and I^- ions, as the complex forms. There have been many investigations, including some recent work, with the continuing goal of identifying the structure of the blue colored iodine starch complex [1–3, 5]. As for the structure of the iodine product formed, a recent study by Madhu et. al. has suggested that the iodine portion of the complex forms an infinite polymeric iodide chain which creates the colored complex upon starch binding [5]. Another study from Yu et. al. suggests that a coexistence of I_3^- and I_5^- is integral to the formation of the complex [26]. The work presented here does indicate that I^-, I_2, and I_3^- are all present as the complex forms and all three should be considered as potential building blocks as the iodine-starch complex is constructed.

As was mentioned earlier, an increase in the alcohol concentration caused a noticeable decrease in the solubility of the starch and the iodine-starch complex. The complex requires a

stable solvation network to remain in solution. However, even when simple alcohols are introduced into the solution, the intermolecular forces weaken to the point of destabilizing the solvation environment of the starch. As was noted prior, the addition of alcohol to the solution could cause significant starch precipitation. The precipitation is caused by the alcohols weakening the solvation network around the starch; thus, the network is more likely to break under the strain from a solvated but constrained starch molecule. Since similar levels of precipitation can occur both prior to and after formation of the iodine-starch complex, the exterior of the iodine-starch complex is composed primarily of starch. This observation supports the basic structure of the product complex that was utilized in other experiments [29, 34].

Combining the laminar flow analysis with the weaker intermolecular forces of the alcohols, it is perhaps unsurprising that there were starch solubility issues with higher concentrations of longer chain alcohols. Both the properties of the alcohols and the potentially unstable solvation environment between different laminar flow planes are conducive to starch and iodine-starch complex precipitation. The solvation environment around both the starch and the complex is easily disrupted and requires a minimum intermolecular force strength to maintain its integrity. In light of these observations the flow analysis for larger ethanol and all 1-propanol concentrations (shown in *Supporting Information*) are more complicated than simple laminar flow due to precipitated starch and product complex causing small regions of turbulence.

3.3 Solvatochromatic Effects

As the solvent composition changes, the wavelength of maximum absorbance of the iodine-starch complex (λ_{max}) also changes. Specifically, as the amount of alcohol increases and/or the alcohol chain length increases, both λ_{max} and the visible light absorbance profile shift toward the blue (Fig. 7). There are two primary aspects of the solvent that are influencing the observed

solvatochromatism in this reaction. First, the concentration of the alcohols in the solvation environment of the iodine-starch complex are reflective of their concentration in the total solvent composition; there is no preferential solvation of the complex. Second, the length of the carbon chain on the alcohol (i.e. the polarity of the alcohol) does have a noticeable effect on the degree of blue shift observed relative to a solvent of only water. The absorbance of the I_3^- does not noticeably shift with changing solvent composition while the I_2 absorbance does shift slightly but it is difficult to observe from the spectra without fitting the absorbances (Fig. 7).

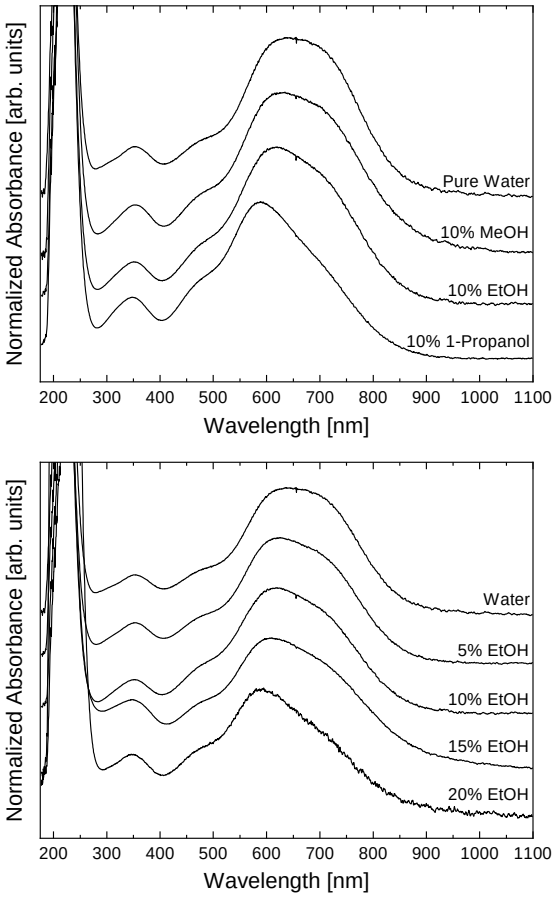

Fig. 7 Product UV-Vis absorption spectra of 10% of each alcohol type (top) and all ethanol compositions (bottom) collected in the final duct of the millifluidic device

In an effort to quantify the effect of different solvent compositions on the spectral signatures of the iodine-starch product, a number of different solvent configurations were tested

(discussed in Experimental Methods). The absorption spectrum of the products for each solvent configuration, collected in the seventh and final duct of the device, was fit with four Gaussian curves: one each for I_3^- and I_2, and two for the visible complex absorption [26]. Yu et. al. showed that there were at least two absorbances present, around 590 nm and 690 nm, in the absorption spectrum of the aqueous complex, however they stated that the exact peak positions were difficult to pinpoint [26]. The results of the peak fitting are shown in Table 2 and details of the Gaussian curve fitting are shown in *Supporting Information*.

Table 2 Solvent compositions (reported in % by volume), solvent polarity (Lewis acidity) [35], and spectral information for each of the solvent mixtures tested. All λ_{max} values were obtained using Gaussian curve fits of the absorption spectra and uncertainties are two standard deviations of the fit λ_{max} value.

	Solvent %	**Polarity**	**I_3^- λ_{max} (nm)**	**I_2 λ_{max} (nm)**	**Complex λ_{max} (nm)**	
Water	N/A	1.00	346.4 ± 0.6	477 ± 1	588.7 ± 0.6	695 ± 2
Methanol	5	0.96	347.1 ± 0.6	476.7 ± 0.8	588.2 ± 0.6	694 ± 2
	10	0.92	348.4 ± 0.4	473.6 ± 0.6	585.1 ± 0.4	686 ± 2
	15	0.90	341.6 ± 0.6	473 ± 1	581.7 ± 0.8	676 ± 3
	20	0.88	343 ± 1	463 ± 2	566 ± 3	650 ± 10
Ethanol	5	0.92	347.0 ± 0.4	474.5 ± 0.8	587.0 ± 0.6	693 ± 2
	10	0.87	346.7 ± 0.4	472.9 ± 0.8	582.6 ± 0.4	685 ± 2
	15	0.82	336.8 ± 0.4	471.2 ± 0.6	576.6 ± 0.6	671 ± 3
	20	0.78	339 ± 1	466 ± 1	572 ± 1	642 ± 6
Propanol	5	0.83	342.8 ± 0.4	469.8 ± 0.8	578.1 ± 0.6	680 ± 2
	10	0.74	343.1 ± 0.4	465.2 ± 0.4	568.7 ± 0.4	657 ± 3
	15	0.70	343.4 ± 0.4	462.7 ± 0.6	563.8 ± 0.6	642 ± 4

As was established in the previous section, the exterior of the complex is composed predominantly of starch so the solvatochromatic shifts are due to interactions between the solvation environment and the starch exterior. Since the starch and iodide do not exhibit any visible absorbance until the complex is formed, the iodine core and its interaction with the starch are clearly integral to the electronic transition(s) that give rise to the color of the complex [13]. However, the chemical interactions between solvent and complex are localized to the external

starch. The observed blue shift of the complex absorbance concomitant with the decreasing polarity of the solvent environment is an example of a bathochromic shift [36]. However, both a decrease in the polarity of the solvent environment and a weakening of the solvation network are possible causes of the shift. Both of these effects can contribute to the destabilization of the ground electronic state and the excited electronic states of the complex responsible for the visible transition with respect to each other. The decreasing polarity can change the orbital energies to different degrees while the weakening solvation network should specifically cause a conformational change of the starch exterior – likely an expansion of the starch away from the iodine core – that could contribute to the observed bathochromic shift.

Figure 8 shows the maxima of the two Gaussian curves fit to the visible absorption of the product complex (in cm^{-1}) plotted against the relative polarity of the solvent. Both maxima exhibit an increasing non-linear relationship for each alcohol tested. Specifically, increasing alcohol concentration corresponds with an increasing blue shift and lengthening the non-polar chain of the alcohol, at a constant concentration, increases the degree of observed blue shift. These observations, again, indicate that the solvation environment is a reflection of the solvent composition as a whole and there does not appear to be preferential solvation of the iodine-starch complex. The alcohols are being inserted into the solvation network around the iodine-starch complex, resulting in interactions that, as described above, destabilize the electronic structure of the iodine-starch complex. It should be noted that the Gaussian fitting was difficult for aqueous 20% methanol and ethanol solutions due to low signal to noise ratios and resulted in substantially larger error bars than in the other fits.

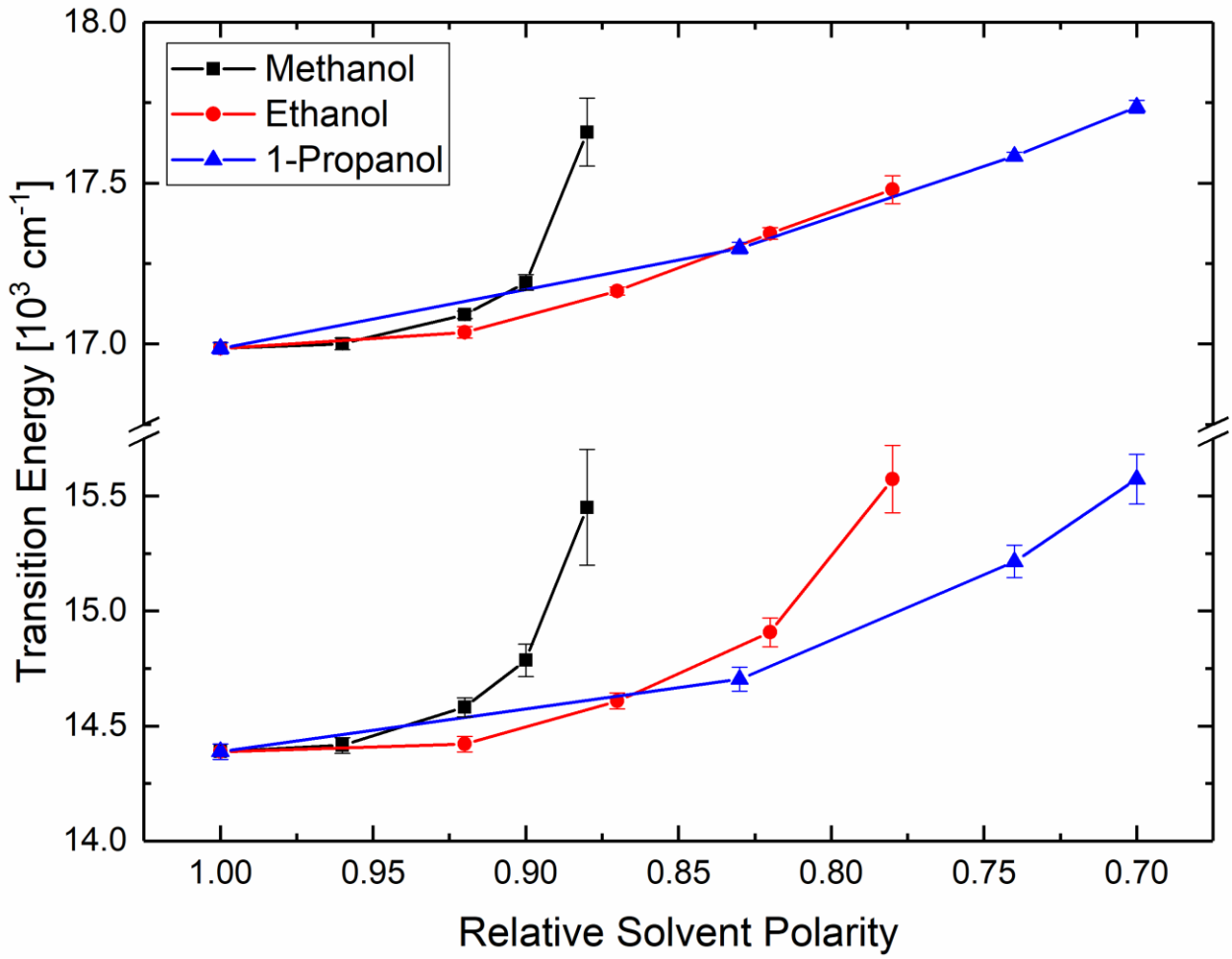

Fig. 8 Frequency of the iodine-starch complex absorption, ca. 650 nm, as a function of relative solvent polarity for methanol (black squares), ethanol (red circles), and 1-propanol (blue triangles) with the λ_{max} of the higher frequency fit peak (~590 nm peak) shown on top and the lower frequency fit peak (~690 nm peak) shown on the bottom, the solid lines are not fits of their respective data sets, the error bars are two standard deviations of the fit λ_{max}

While this work cannot solve for the exact structure of the iodine-starch complex, some insight can be gained based on the effect of the solvation environment on the product. As has already been noted, the ability of the complex to form does not appear to be noticeably affected by the presence or lack of alcohol. The longer the carbon chain on the alcohol, the larger the observed solvatochromatic shift, which follows the same trend as the decreasing dielectric constant of each alcohol (dielectric constants in units of relative permittivity for the four solvents are: water = 80.37 at 20 ˚C, methanol = 32.35 at 20 ˚C, ethanol = 25.00 at 20 ˚C, 1-propanol = 20.50 at 25 ˚C) [37,

38]. However, it has been established that the polarity (Lewis acidity) of an aqueous solution often does not change linearly with changing cosolvent concentration due to the highly polar and structured nature of liquid water [35, 36]. This is true for aqueous solutions of methanol, ethanol, and 1-propanol (see Table 2). For all three alcohols the polarity of the solution decreases quickly with the initial addition of alcohol and then decreases at a slower rate as the alcohol concentration increases further [35]. This effect is more pronounced as the alcohol chain length increases [35]. The trend in solution polarity is mirrored in the slight blue shift of the I_2 absorbance but not in the absorbances of the product complex. The blue shifts observed in Fig. 8 do not exhibit a large initial shift that becomes smaller as the alcohol concentration increases, concomitant with the polarity of the solution, but rather the opposite. The degree of blue shift mostly increases with increasing alcohol concentration. It follows that the dominant cause of the observed shifts is the weakening of the solvation network, not the decreasing solvent polarity. The weakening of the solvation shell is most pronounced in the relatively large 1-propanol shifts where it has been stated previously that the solubility of the starch was already decreased even at low concentrations of 1-propanol. If the polarity of the solvent were the dominant effect, the observed shifts should be more linear when plotted against the solution polarity [35, 36]. It would also be expected that solutions with similar polarities would exhibit similar blue shifts which is not observed in Fig. 8. While the decreasing polarity of the solvent may contribute some to the bathochromic shifts, the increasing shifts seen in Fig. 8 suggest it is a secondary effect to the weakening of the solvation network around the complex. The solvent shell appears to be an integral component to the geometric and electronic structure of the complex and solvation properties need to be considered when attempting to describe or model the complex.

The excited states of the transitions are affected differently by the changes in the solvent environment, since the two absorbances that make up the large 650 nm feature do not blue shift at the same rate (Fig. 8). The area and height parameters of the curve fitting show two trends of the 590 nm and 690 nm peaks. When the alcohol concentration increases, the 590 nm peak becomes less intense relative to the 690 nm peak indicating that the weakening solvation environment is more disruptive of the intensity of the 590 nm transition. However, when the alcohol chain length is increased at a given solvent polarity the 590 nm peak becomes more intense relative to the 690 nm peak (see *Supporting Information:* Table S4 for fit parameters). In all solvents the 690 nm peak is the dominant transition. The 590 nm peak appears to respond more in alignment to the polarity of the solvation environment than the 690 nm peak, which is primarily shifted by the weakening of the solvation network and conformational change of the complex. Based on the trends in the amplitude and area of the peaks, the 590 nm transition appears to depend more on orbitals localized on the starch exterior while the 690 nm transition is primarily governed by the orientation of the starch around the iodine core. These differences in response to the changing solvent environment are visible in Fig. 8 where the 590 nm and the 690 nm peak trends, with the exception of the 590 nm peak in 20% methanol, show different trajectories. This data creates benchmarks for the expected properties of the electronic states of the iodine-starch complex under various solvent configurations. These spectra should create a reference point for substantial computational studies concerning the nature of the iodine-starch complex when subjected to various solvent environments.

4 Conclusion

The iodine clock reaction and its dark blue colored product has been an elusive target of chemists for many years. The work presented here showed a unique spectroscopic approach toward probing the reaction as it evolved, allowing for spectra to be acquired as the reaction progressed. The results indicate that the iodine-starch complex resides in solution where there is a stable solvation environment and decreases in the polarity of the solvent environment result in a conformational change to the iodine-starch complex and a decreased solubility. Additionally, when the solvent environment weakens, the conformational change in the complex causes a noticeable blue shift in the absorbance frequencies of the two visible electronic transitions. The two transitions of the complex exhibit blue shifts at different rates caused primarily by the weakening solvation environment and, as a secondary effect, the decreasing polarity of the solvent. These results indicate that the solvent shell is an integral part of the blue iodine-starch complex and contributes to the electronic transitions. The observations presented here give benchmarks for the physical and electronic structure of the iodine-starch complex and some of the solvation considerations that should be made when trying to model the complex.

Further studies of the iodine-clock reaction with other solvents, such as glycerin or ethylene glycol, which can dissolve in water, maintain starch solubility, and possess polarities outside of the range of the alcohols studied here could expand upon some of the solvent-complex interactions presented. Raman spectroscopy may also be a useful technique to employ in elucidating the nature of the iodine species in the final product complex as it forms over time and in different solvent environments.

Associated Content:

The following files are available free of charge.

Supporting Information - Additional experimental and flow modeling details, waterfall spectra for all solvent configurations, absorbances as a function of elapsed reaction time, and Gaussian fits with their fitting parameters for Fig. 8. (docx)

3D model (.dwg) and printing (.stl) files for the millifluidic devices used. (dwg) (stl)

References:

1. Thoma, J.A., French, D.: Studies on the Schardinger dextrins. X. The Interaction of Cyclohexaamylose, Iodine and Iodide. Part I. Spectrophotometric Studies. J. Am. Chem. Soc. **80**, 6142–6146 (1958)
2. Thoma, J.A., French, D.: The Starch-Iodine-Iodide Interaction. Part I. Spectrophotometric Investigations. J. Am. Chem. Soc. **82**, 4144–4147 (1960)
3. Teitelbaum, R.C., Ruby, S.L., Marks, T.J.: A Resonance Raman/Iodine Mossbauer Investigation of the Starch-Iodine Structure. Aqueous Solution and Iodine Vapor Preparations. J. Am. Chem. Soc. **102**, 3322–3328 (1980)
4. Lambert, J.L., Fina, G.T.: Iodine clock reaction mechanisms. J. Chem. Educ. **61**, 1037–1038 (1984)
5. Madhu, S., Evans, H.A., Doan-Nguyen, V.V.T., Labram, J.G., Wu, G., Chabinyc, M.L., Seshadri, R., Wudi, F.: Infinite Polyiodide Chains in the Pyrroloperylene-Iodine Complex: Insights into the Starch-Iodine and Perylene-Iodine Complexes. Angew. Chem. Int. Ed. Engl. **55**, 8032 (2016)
6. Landolt, H.: Ueber die Zeitdauer der Reaction zwischen Jodsäure und schwefliger Säure. Eur. J. Inorg. Chem. **19**, 1317–1365 (1886)
7. Landolt, H.: Ueber die Zeitdauer der Reaction zwischen Jodsäure und schwefliger Säure. Eur. J. Inorg. Chem. **20**, 745–760 (1887)
8. Briggs, T.S., Rauscher, W.C.: An Oscillating Iodine Clock. J. Chem. Educ. **50**, 496 (1973)
9. Shakhashiri, B.Z.: Chemical Demonstrations - Volume 2. University of Wisconsin Press, Madison (1985)
10. Saenger, W.: The Structure of the Blue Starch-Iodine Complex. Naturwissenschaften **71**, 31–36 (1984)
11. Awtrey, A.D., Connick, R.E.: The Absorption Spectra of I_2, I_3^-, I^-, IO_3^-, $S_4O_6^-$ and $S_2O_3^-$. Heat of the Reaction $I_3^- = I_2 + I^-$. J. Am. Chem. Soc. **73**, 1842–1843 (1951)
12. Robin, M.B.: Optical Spectra of Benzamide–Triiodide Ion Complexes : A Model of the Starch–Iodine Complex. J. Chem. Phys. **40**, 3369 (1964)
13. Takashi, H., Hirofumi, Y., Tadahiro, I., Takeshi, N.: Deep Blueing Mechanism of Triiodide Ions in Amylose Being Associated with Its Conformation. In: ACS Symposium Series, Vol. 150. pp. 455–475 (1981)
14. Kloo, L., Rosdahl, J., Svensson, P.H.: On the Intra- and Intermolecular Bonding in Polyiodides. Eur. J. Inorg. Chem. **5**, 1203–1209 (2002)
15. Warshel, A.: Calculations of Chemical Processes in Solutions. J. Phys. Chem. **83**, 1640–1652 (1979)
16. Seely, G.R., Jensen, R.G.: Effect of Solvent on the Spectrum of Chlorophyll. Spectrochim. Acta **21**, 1835–1845 (1965)
17. Bakhshiev, N.G.: Universal Molecular Interactions and their effect on the Position of the Electronic Spectra of Molecules in two-component Solutions. Opt. Spectrosc. **10**, 379–384

(1961)
18. Bayliss, N.S.: The Effect of the Electrostatic Polarization of the Solvent on Electronic Absorption Spectra in Solution. J. Chem. Phys. **18**, 292–296 (1950)
19. Bayliss, N.S., Hulme, L.: Solvent Effects in the Spectra of Benzene, Toluene, and Chlorobenzene at 2600 and 2000 Å. Aust. J. Chem. **6**, 257–277 (1953)
20. Brooker, L.G.S., Keyes, G.H., Sprague, R.H., VanDyke, R.H., VanLare, E., VanZandt, G., White, F.L., Cressman, H.W.J., Dent, S.G.: Color and Constitution. X.1 Absorption of the Merocyanines2. J. Am. Chem. Soc. **73**, 5332–5350 (1951)
21. McRae, E.G.: Theory of Solvent Effects on Molecular Electronic Spectra. Frequency Shifts. J. Phys. Chem. **61**, 562–572 (1957)
22. Luzhkov, V., Warshel, A.: Microscopic Models for Quantum Mechanical Calculations of Chemical Processes in Solutions: LD/AMPAC and SCAAS/AMPAC Calculations of Solvation Energies. J. Comput. Chem. **13**, 199–213 (1992)
23. Bader, J.S., Cortis, C.M., Berne, B.J.: Solvation and Reorganization Energies in Polarizable Molecular and Continuum Solvents. J. Chem. Phys. **106**, 2372–2387 (1997)
24. Renger, T., Grundkotter, B., Madjet, M.E.-A., Muh, F.: Theory of solvatochromic shifts in nonpolar solvents reveals a new spectroscopic rule. Proc. Natl. Acad. Sci. **105**, 13235–13240 (2008)
25. Baldwin, R.R., Bear, R.S., Rundle, R.E.: The Relation of Starch-Iodine Absorption Spectra to the Structure of Starch and Starch Components. J. Am. Chem. Soc. **66**, 111–115 (1944)
26. Yu, X., Houtman, C., Atalla, R.H.: The Complex of Amylose and Iodine. Carbohydr. Res. **292**, 129–141 (1996)
27. Stamixco: Helical Static Mixer (Type HT), http://www.stamixco-usa.com/helical
28. Summerlin, L.R., Ealy Jr, J.L.: Chemical Demonstrations: A Sourcebook for Teachers Volume 1. American Chemical Society (1988)
29. Miller-Chou, B.A., Koenig, J.L.: A Review of Polymer Dissolution. Prog. Polym. Sci. **28**, 1223–1270 (2003)
30. Stone, H.A.: Introduction to Fluid Dynamics for Microfluidic Flows. In: Lee, H., Ham, D., and Westervelt, R.M. (eds.) CMOS Biotechnology. pp. 5–30. Springer US (2007), Chap 1
31. Spiga, M., Morini, G.L.: A Symmetric Solution for Velocity Profile in Laminar Flow through Rectangular Ducts. Int. Commun. Heat Mass Transf. **21**, 469–475 (1994)
32. Palmer, D.A., Ramette, R.W., Mesmer, R.E.: Triiodide Ion Formation Equilibrium and Activity Coefficients in Aqueous Solution. J. Sol. Chem. **13**, 673–683 (1984)
33. Morrison, M., Bayse, G.S., Michaels, A.W.: Determination of Spectral Properties of Aqueous I_2 and I_3^- and the Equilibrium Constant. Anal. Biochem. **42**, 195–201 (1971)
34. Swanson, M.A.: Studies on the Structure of Polysaccharides IV. Relation of the Iodine Color to the Structure. J. Biol. Chem. **172**, 825–837 (1948)
35. Krygowski, T.M., Wrona, P.K., Zielkowska, U., Reichardt, C.: Empirical Parameters of Lewis Acidity and Basicity for Aqueous Binary Solvent Mixtures. Tetrahedron. **41**, 4519–4527 (1985)
36. Reichardt, C.: Solvatochromic Dyes as Solvent Polarity Indicators. Chem. Rev. **94**, 2319–2358 (1994)
37. Åkerlöf, G.: Dielectric Constants of some Organic Solvent-Water Mixtures at Various Temperatures. J. Am. Chem. Soc. **54**, 4125–4139 (1932)
38. 1-Propanol. SDS Methanol. 1–6 (2018)

TOC Image:

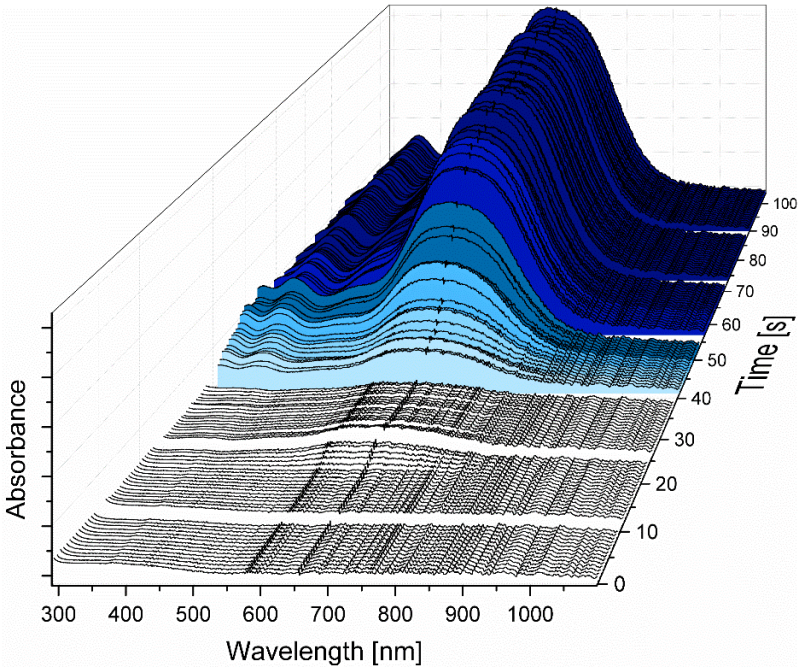
Absorbance
Wavelength [nm]
300
400
500
600
700
800
900
1000
Time [s]
0
10
20
30
40
50
60
70
80
90
100